


Article

Elaboration of Highly Modified Stainless Steel/Lead Dioxide Anodes for Enhanced Electrochemical Degradation of Ampicillin in Water

Yasmine Ben Osman ^{1,2,3,4}, Samar Hajjar-Garreau ^{3,4}, Dominique Berling ^{3,4}  and Hanene Akrouit ^{1,*}

¹ Laboratory of Wastewaters and Environment, Center of Water Researches and Technologies (CERTE) Technopark of Borj Cedria, PB 273, Soliman 8020, Tunisia

² National Institute of Applied Sciences and Technology (INSAT), University of Carthage, BP 676, Tunis 1080, Tunisia

³ CNRS, IS2M UMR 7361, Université de Haute-Alsace, 68100 Mulhouse, France

⁴ CNRS, UMR 7361, Université de Strasbourg, 67000 Strasbourg, France

* Correspondence: hanene.akrouit@gmail.com

Abstract: Lead dioxide-based electrodes have shown a great performance in the electrochemical treatment of organic wastewater. In the present study, modified PbO₂ anodes supported on stainless steel (SS) with a titanium oxide interlayer such as SS/TiO₂/PbO₂ and SS/TiO₂/PbO₂-10% Boron (B) were prepared by the sol-gel spin-coating technique. The morphological and structural properties of the prepared electrodes were characterized by scanning electron microscopy (SEM), energy-dispersive X-ray spectroscopy (EDX), and X-ray photoelectron spectroscopy (XPS). It was found that the SS/TiO₂/PbO₂-10% B anode led to a rougher active surface, larger specific surface area, and therefore stronger ability to generate powerful oxidizing agents. The electrochemical impedance spectroscopy (EIS) measurements showed that the modified PbO₂ anodes displayed a lower charge transfer resistance R_{ct}. The influence of the introduction of a TiO₂ intermediate layer and the boron doping of a PbO₂ active surface layer on the electrochemical degradation of ampicillin (AMP) antibiotic have been investigated by chemical oxygen demand measurements and HPLC analysis. Although HPLC analysis showed that the degradation process of AMP with SS/PbO₂ was slightly faster than the modified PbO₂ anodes, the results revealed that SS/TiO₂/PbO₂-10%B was the most efficient and economical anode toward the pollutant degradation due to its physico-chemical properties. At the end of the electrolysis, the chemical oxygen demand (COD), the average current efficiency (ACE) and the energy consumption (EC) reached, respectively, 69.23%, 60.30% and 0.056 kWh (g COD)⁻¹, making SS/TiO₂/PbO₂-10%B a promising anode for the degradation of ampicillin antibiotic in aqueous solutions.



Citation: Ben Osman, Y.; Hajjar-Garreau, S.; Berling, D.; Akrouit, H. Elaboration of Highly Modified Stainless Steel/Lead Dioxide Anodes for Enhanced Electrochemical Degradation of Ampicillin in Water. *Separations* **2023**, *10*, 5. <https://doi.org/10.3390/separations10010005>

Academic Editors:

Dimosthenis Giokas and
Manolis Manos

Received: 18 November 2022

Revised: 11 December 2022

Accepted: 13 December 2022

Published: 22 December 2022



Copyright: © 2022 by the authors. Licensee MDPI, Basel, Switzerland. This article is an open access article distributed under the terms and conditions of the Creative Commons Attribution (CC BY) license (<https://creativecommons.org/licenses/by/4.0/>).

Keywords: lead dioxide; titanium dioxide; boron doping; anodic oxidation; ampicillin removal

1. Introduction

The presence of antibiotics in the aqueous ecosystem represents nowadays an emerging concern since it can be a real threat on human health, aquatic life, and plants [1]. The main sources of the pharmaceuticals detected in the environment are domestic sewage, hospital effluents and pharmaceutical manufacturing companies [2]. Therefore, it is necessary to develop an effective treatment to remove these emerging organic pollutants from wastewaters in order to prevent their presence in natural water receptors.

Over the last few decades, advanced oxidation processes (AOPs) were proposed as the most promising technologies for antibiotic removal from the environment since the conventional methods are no more efficient. Anodic oxidation (AO) stands out among the most promising AOPs to treat refractory pharmaceutical compounds owing to its simple, safe, economic and environmentally compatible technology [3–6].

The AO process is based on the degradation of persistent organic pollutants with highly reactive hydroxyl radicals (OH^\bullet) produced at the anode surface [7–9]. The efficiency of the generated hydroxyl radicals depends mainly on the anode materials in terms of composition and morphology [10,11]. Lead dioxide (PbO_2) is among the widely used anodes for wastewater treatment thanks to its high electrical conductivity, good stability, low cost and long service lifetime [8,12,13]. However, the fragile binding force and the low stability of PbO_2 coating may lead to lead ions leaching during the electrolysis process, or it could even peel off of the coating from the substrate surface, affecting therefore the lifetime of the electrode and limiting its practical application [14].

Therefore, further improvements are required to enhance the electrode efficiency for organic pollutants degradation. Over the past decades, research focused on PbO_2 coating modification and its subsequent effects on the active layer performance [15–18].

Conventional PbO_2 anodes were modified by the introduction of a conductive intermediate layer which contributed to prolonging the service life, minimizing the lead ions leaching and improving the oxidation effectiveness and current efficiency of lead dioxide electrodes [19–21]. For example, silicon dioxide (SiO_x) thin film was used by Elaissaoui et al. as an interlayer in order to improve the SS/ PbO_2 anode efficiency and stability for dye removal [22]. Duan and co-workers reported that the deposition of a carbon nanotube interlayer increased the service lifetime and promoted the oxidation capacity of pure PbO_2 electrodes for 4-chlorophenol degradation [23]. Tin dioxide (SnO_2) is also among the added metal oxides allowed to reach high degradation rates [24,25] as well as manganese dioxide (MnO_2) [26] and titanium dioxide (TiO_2) [27–29] interlayers used to improve the electrochemical oxidation treatments of refractory organic wastewater, respectively, by strengthening the bonding between the substrate and the active outer layer which increases, therefore, the anode's electrical conductivity.

Furthermore, doping the PbO_2 layer has also been extensively adopted as an effective modification method to promote the electrocatalytic characteristics and improve the stability of PbO_2 -based electrodes [19]. Several elements such as indium [30], cobalt [31], copper [32] and aluminum [33] were used as dopants to enhance the oxidizing power of lead dioxide anode since dopant introduction provides a larger active surface area, higher oxygen evolution potential, and lower charge transfer resistance [8,15].

However, to the best of our knowledge, there are no reports about PbO_2 anodes modified by boron (B). Only boron-doped diamond (BDD) electrodes were used, in recent years, and considered as an optimal electrode material for the electrochemical oxidation of organic pollutants in the wastewater system thanks to their physical and chemical properties [34,35] and the distribution of sp^2 carbon impurities on the anode surface that influences the electrocatalytic properties [36].

The aim of the current research is to improve the electrocatalytic activity and stability of the PbO_2 electrode by (i) the introduction of a TiO_2 inner layer between the stainless steel substrate and the outer coating and (ii) the combination of the high activity of boron and the lead oxide in order to develop SS/ TiO_2 / PbO_2 -B anode using sol-gel spin coating. This study aligns with the overall goal of the InTheMED project aiming to develop and to implement low-cost sustainable remediation strategies. The main purposes of this work were (i) to remove residual antibiotics from wastewater, (ii) to contribute to increasing the safe reuse of treated effluent and (iii) to preserve the MED aquifers to mitigate anthropogenic threats in changing climate.

The physicochemical and morphological properties of SS/ TiO_2 / PbO_2 and SS/ TiO_2 / PbO_2 -B electrodes were characterized by scanning electron microscopy (SEM), energy-dispersive X-ray spectroscopy (EDX), and X-ray photoelectron spectroscopy (XPS). The understanding of electric properties was performed by the electrochemical impedance spectroscopy measurements (EIS) and compared with those of the conventional SS/ PbO_2 anodes. Ampicillin (AMP) was selected as a pharmaceutical pollutant model since it is one of the most commonly detected antibiotics in wastewater in several countries [37]. According to recent studies, AMP was detected in Kenya [38] and Czech Republic wastewater at a concentration of 28.09 ng/L [39], and

also, concentrations ranging from 0.012 to 32.57 $\mu\text{g}/\text{mL}$ were reported in Pakistan [40]. The electrocatalytic activity of the developed anodes was investigated during the anodic oxidation of AMP in synthetic wastewater. The mineralization of the organic matter and the concentration of ampicillin were, respectively, evaluated by chemical oxygen demand and high-performance liquid chromatography analysis.

2. Materials and Methods

2.1. Chemicals

Titanium isopropoxyde (TTIP, $\text{Ti}(\text{OCH}(\text{CH}_3)_2)_4$, Sigma-Aldrich, 97% purity) was used as a precursor for TiO_2 interlayer deposition. Lead(II) acetate trihydrate ($\text{Pb}(\text{C}_2\text{H}_3\text{O}_2)_2$, Assay $\geq 99\%$, $379.33 \text{ g mol}^{-1}$), methacrylic acid (MAA: $\text{H}_2\text{C}=\text{C}(\text{CH}_3)\text{COOH}$, Assay $\geq 99\%$, 86.09 g mol^{-1}), hydrochloric acid (HCl, 37%, 36.46 g mol^{-1}) and 1-propanol ($\text{CH}_3\text{CH}_2\text{CH}_2\text{OH}$, Assay $\geq 99.7\%$, 60.10 g mol^{-1}) were used for PbO_2 deposition. Boric acid (H_3BO_3 , Sigma-Aldrich, $\geq 99.5\%$ purity, 61.83 g mol^{-1}) was used as dopant. Sodium sulfate (Na_2SO_4 , $142.04 \text{ g mol}^{-1}$, LOBA chemie) was used as supporting electrolyte during the electrochemical measurements and the degradation experiment. Potassium dihydrogen phosphate (KH_2PO_4 , $136.086 \text{ g mol}^{-1}$) and methanol (HPLC grade) were used for chromatographic analysis. Acetone (CH_3COCH_3 , 58.01 g mol^{-1}) was used to clean the substrates. Ampicillin antibiotic ($\text{C}_{16}\text{H}_{18}\text{N}_3\text{NaO}_4\text{S}$, FLUKA Chemie, $371.39 \text{ g mol}^{-1}$) was used as an organic pollutant.

2.2. Preparation of Modified PbO_2 Electrodes

Stainless steel-AISI 304 plates were used as substrates. The electrodes were, first, polished with abrasive paper with different roughness ranging from 320 to 1200, degreased in acetone for 10 min using an ultrasonic bath (Ultrasonic Batch-FALC), rinsed with distilled water and finally dried under nitrogen flow.

The PbO_2 electrodes were prepared by the sol-gel spin-coating technique. Concerning the titanium oxide interlayer, TiO_2 sol gel solution was prepared by mixing 2 mL of methacrylic acid and 1 mL of titanium isopropoxyde for 5 min; then, 0.5 mL of propanol was added to the mixture and stirred for 10 min. Finally, 0.9 mL of 0.37 M HCl was added, and the solution was stirred for 1 h. The TiO_2 interlayer was spin coated at 1000 rpm during one minute and annealed at 600°C for 1 h in order to evaporate the solvents.

The PbO_2 solution was synthesized by dissolving 1.28 g of lead acetate in methacrylic acid, 1-propanol and 0.37 M HCl. The solution was stirred for 1 h. For the boron (B)-doped anode, 0.023 g of boric acid (H_3BO_3) was added with 10% mass percentage during the first step of Pb precursor solution formulation. The B doping rate was chosen based on the work of Boukhchina et al. [41]. Small droplets of the un-doped and doped PbO_2 were deposited on a TiO_2 layer that was then spun at 2000 rpm for 60 s. Five thin films of PbO_2 were deposited layer by layer to obtain a final thickness around 1000 nm, and the coating was finally dried at 200°C for 24 h on a hot plate as described in Figure 1. In order to obtain the optimized thickness of the TiO_2 and PbO_2 layer, the rotation speed, the number of the deposited layers and the annealing temperature were varied, and the thicknesses of the films were measured after each test in order to determine the appropriate parameters [42].

2.3. Electrode Characterizations

2.3.1. Electrode Morphology and Composition

The morphology of the deposited films was examined by scanning electron microscopy (SEM, FEI quantum 400 FEG Electron Microscope). An energy-dispersive X-ray analysis (EDX) is included in this instrument for elemental analysis. The composition and chemical state of the modified PbO_2 anodes were investigated using X-ray photoelectron spectrometry (XPS) analysis. The XPS analysis was performed via a VG Scienta SES 2002 spectrometer equipped with a monochromatized Al $K\alpha$ X-ray source (1486.6 eV) and hemispherical analyzer. The analyzed surface area was 24 mm^2 . The high-resolution spectra and wide scan were recorded with a pass energy of 100 eV and 500 eV.

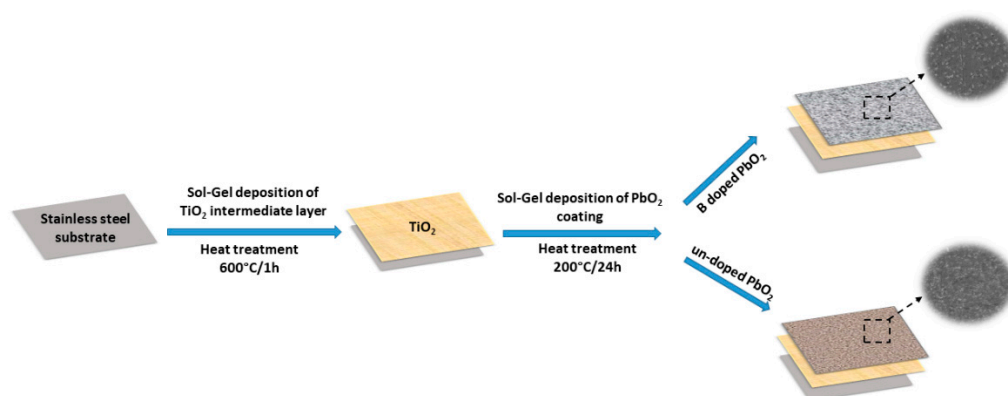


Figure 1. Preparation process of undoped and B doped SS/TiO₂/PbO₂ anode.

2.3.2. Electrochemical Properties

The electrochemical behaviors of PbO₂ anodes were characterized by electrochemical impedance spectroscopy (EIS). EIS measurements were carried out in a conventional three-electrode cell system containing 0.1 M Na₂SO₄ using a VoltaLab PGZ301 potentiostat. PbO₂ anodes were used as the working electrodes, platinum wire was used as the counter electrode, and a saturated calomel electrode was used as the reference electrode. Impedance spectra were recorded in a frequency range varying from 100 kHz to 100 mHz. The experimental data were fitted using ZsimpWin 3.2 software.

2.4. Anodic Oxidation of Ampicillin

2.4.1. Electrolysis

The electrochemical degradation of AMP was carried out in a glass reactor containing 105 mg L⁻¹ of ampicillin and 0.1 M of Na₂SO₄ used as a supporting electrolyte at pH = 4. The SS/PbO₂, SS/TiO₂/PbO₂ and SS/TiO₂/PbO₂-10%B electrodes were prepared and used as anodes with an effective area of 4 cm². An SS plate with the same size was used as the cathode and was supported vertically and parallel to the working anode. The solution was magnetically stirred by a magnetic stirrer during the electrolysis process, and the anodic oxidation of ampicillin was performed under galvanostatic mode at a constant current density of 50 mA cm⁻² for 5 h (Figure 2).

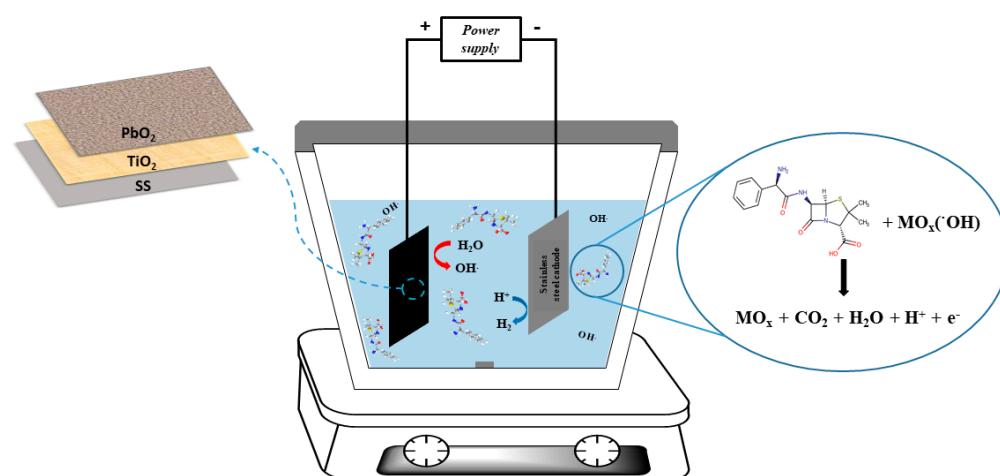


Figure 2. Schematic representation of the electrolysis experimental setup.

2.4.2. Analytical Methods and Evaluation of Degradation Efficiency

The concentration of AMP was determined at different instants during the electrolysis by high-performance liquid chromatography (HPLC). HPLC analysis was carried out using an Agilent technology instrument 1260 infinity II equipped with a thermo-scientific

LC18 column Zorbax eclipse XDB (250 mm × 4.6 mm × 5 μm) used as stationary phase and coupled with a diode strip detector set at the detection wavelength of ampicillin ($\lambda = 204$ nm). The mobile phase is a mixture of methanol: 0.05 M KH_2PO_4 (40:60 *v/v*) flowing through the column at a constant flow rate of 1.0 mL min^{-1} . The mobile phase was filtered through 0.45 μm Millipore filter. The injection volume of AMP was 20 μL.

To assess the mineralization of AMP in solution, the Chemical Oxygen Demand (COD) was determined using the reactor digestion method based on oxidizing the organic matter present in water with an excess of potassium dichromate. The quantity of potassium dichromate used in the reaction is equivalent to the oxygen used to oxidize the organic matter of wastewater. This measurement is carried out according to the French water quality standard protocol (NF T 90-101), and the COD is expressed in mg L^{-1} [43]. The COD removal rate is calculated from the following equation:

$$\text{COD removal(\%)} = \frac{\text{COD}_0 - \text{COD}_t}{\text{COD}_0} \times 100 \quad (1)$$

where COD_0 and COD_t are, respectively, the COD of initial concentration and the COD at given time t .

The average current efficiency (ACE) representing the proportion of the generated radicals serving to oxidize the AMP is determined from COD values (in $\text{gO}_2 \text{L}^{-1}$) using this expression [44]:

$$\text{ACE(\%)} = \frac{(\text{COD}_0 - \text{COD}_t) \times F \times V}{8 \times I \times t} \times 100 \quad (2)$$

where F is the Faraday constant ($96,487 \text{ C mol}^{-1}$), V is the solution volume (L), 8 is the oxygen equivalent mass (g eq^{-1}), I is the applied current (A), and t is the electrolysis time (s).

The electric energy needed to degrade AMP at a given time “ t ” was estimated by calculating the energy consumption per amount of degraded COD ($\text{kWh}(\text{g COD})^{-1}$) according to the following formula [45]:

$$\text{EC}(\text{kWh}(\text{g COD})^{-1}) = \frac{I \times E \times t}{\Delta\text{COD} \times V} \quad (3)$$

where I (0.2 A) is the applied current flowing between the anode and cathode, E is the average cell voltage, t is the electrolysis time, ΔCOD is the decay in COD (mg L^{-1}), and V is the volume of the treated solution (L).

3. Results and Discussion

3.1. Morphological and Structural Characterization of the Anodes Surface

3.1.1. SEM and EDX Analysis

Figure 3 shows SEM micrographs of PbO_2 coating before and after the addition of the TiO_2 interlayer, respectively, in Figure 3a,b. The boron doping of the outer layer is represented in Figure 3c. The addition of the TiO_2 interlayer affects significantly the coating morphology. We notice as depicted in Figure 3b that the anode surface with the TiO_2 interlayer became rougher compared to the SS/ PbO_2 (Figure 3a) directly coated anode surface, which looks more homogeneous and uniform. In comparison with the undoped PbO_2 coating, the incorporation of boron into the PbO_2 coating (Figure 3c) led to a rougher and a more heterogeneous surface covered with small-sized lead dioxide particles. The rough structure obtained with SS/ TiO_2 / PbO_2 and SS/ TiO_2 / PbO_2 -10%B anodes increases the active surface area which provides more active sites for electrochemical reactions and facilitates, thus, the degradation of the pollutant [13,46].

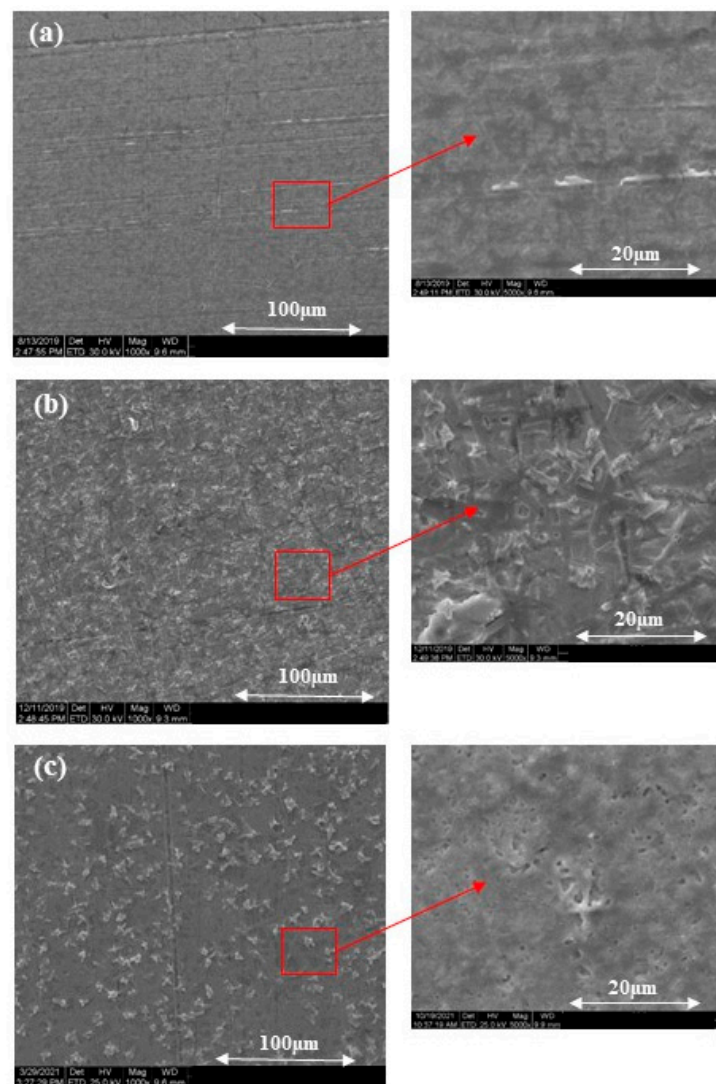


Figure 3. SEM micrographs of (a) SS/PbO₂, (b) SS/TiO₂/PbO₂ and (c) SS/TiO₂/PbO₂-10%B electrodes surface.

According to EDX images of SS/TiO₂/PbO₂ anode in a cross-section (Figure 4), the anode was developed on a silicon substrate, since it is easily breakable compared to the SS substrate. The cross-section images allowed us to check the TiO₂ intermediate layer and the PbO₂ outer layer thicknesses corresponding, respectively, to (112 ± 25) nm and (1000 ± 25) nm after heat treatment.

EDX analysis was carried out to determine the chemical composition of the anodes. From the EDX element mappings of Si/TiO₂/PbO₂ (Figure 4) and SS/TiO₂/PbO₂-10%B (Figure 5) electrodes, we notice that lead (Pb), titanium (Ti) and oxygen (O) are the main detected elements. The homogeneous distribution of Ti and O confirms that the intermediate layer of TiO₂ covers the entire surface of the stainless steel substrate and the Pb distributed in the form of small crystals over the anode surface demonstrates the successful deposition of the PbO₂ active layer.

3.1.2. XPS Analysis

To further study the elementary composition and the chemical environment of SS/TiO₂/PbO₂ and SS/TiO₂/PbO₂-10%B anodes, the electrodes surfaces were investigated by XPS.

The XPS spectrum presented in Figure 6a reveals that Pb and O are the main elements present on the surface of both electrodes and are associated to the PbO₂ film. The detected

carbon (C) is attributed to the anode surface pollution. Since the PbO₂ layer is too thick, the Ti of the intermediate layer does not appear in the XPS spectrum. The boron present in SS/TiO₂/PbO₂-10%B anode is also not observed because of the small relative sensitivity factor (RSF) cross-section of the B1s orbital (B1s = 0.486). In order to quantify the chemical nature of the elements present, high-resolution XPS spectra of Pb and O were measured, and the main results are summarized in Table 1.

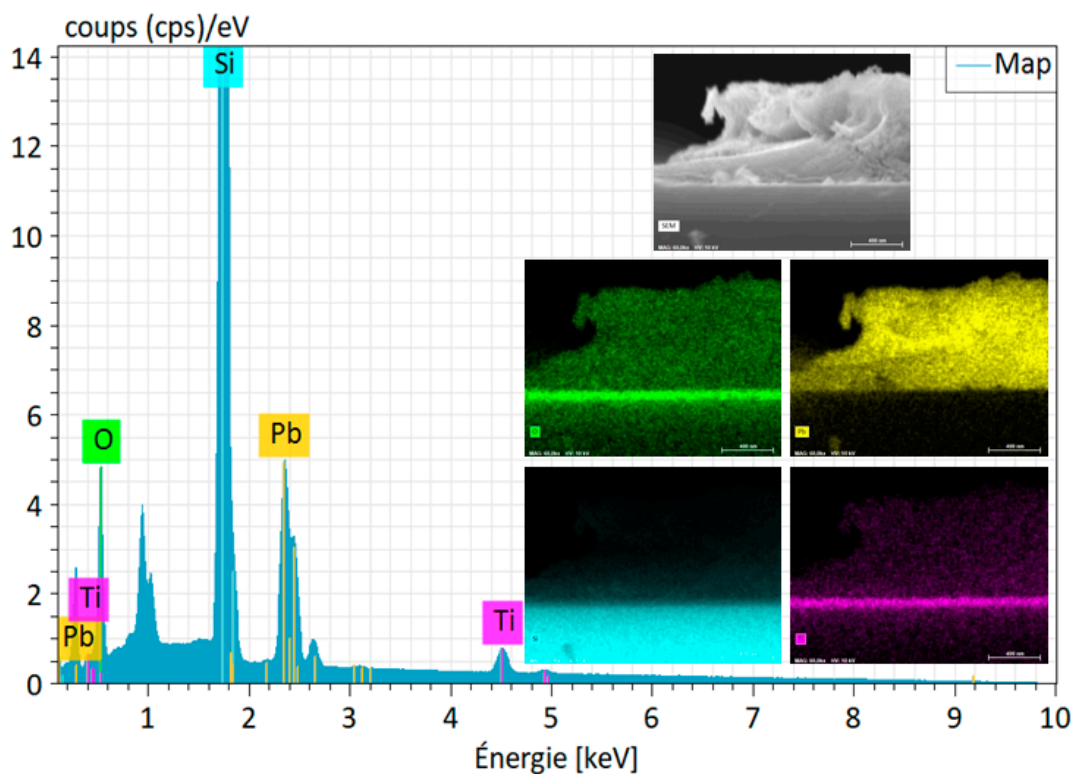


Figure 4. EDX analysis of Si/TiO₂/PbO₂ electrode in cross-section.

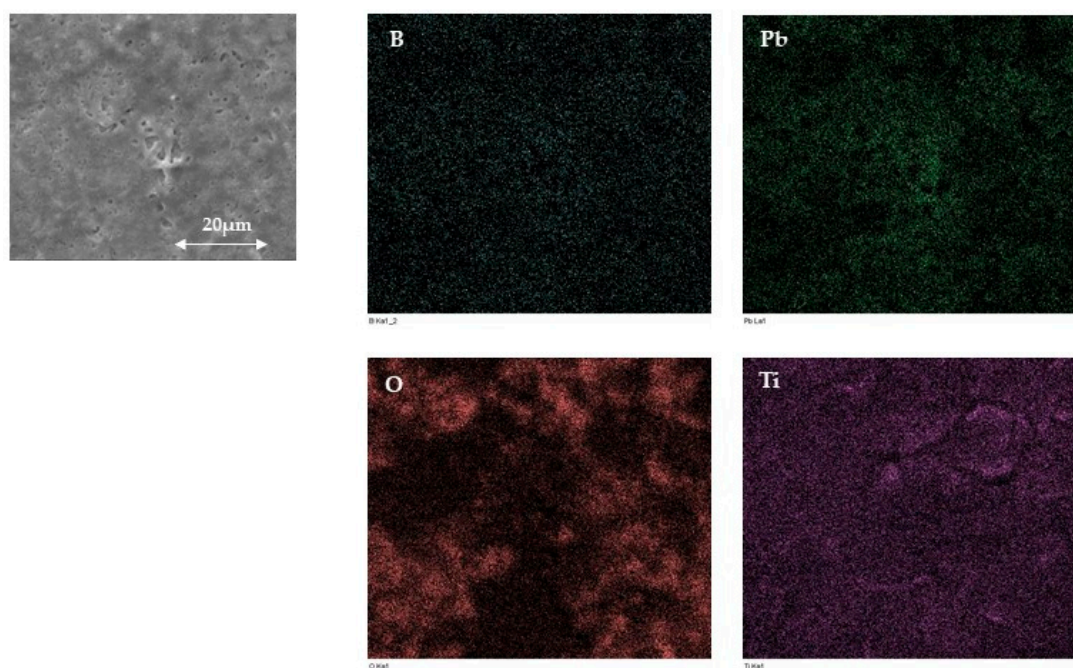


Figure 5. EDX images of SS/TiO₂/PbO₂-10%B electrode in top view.

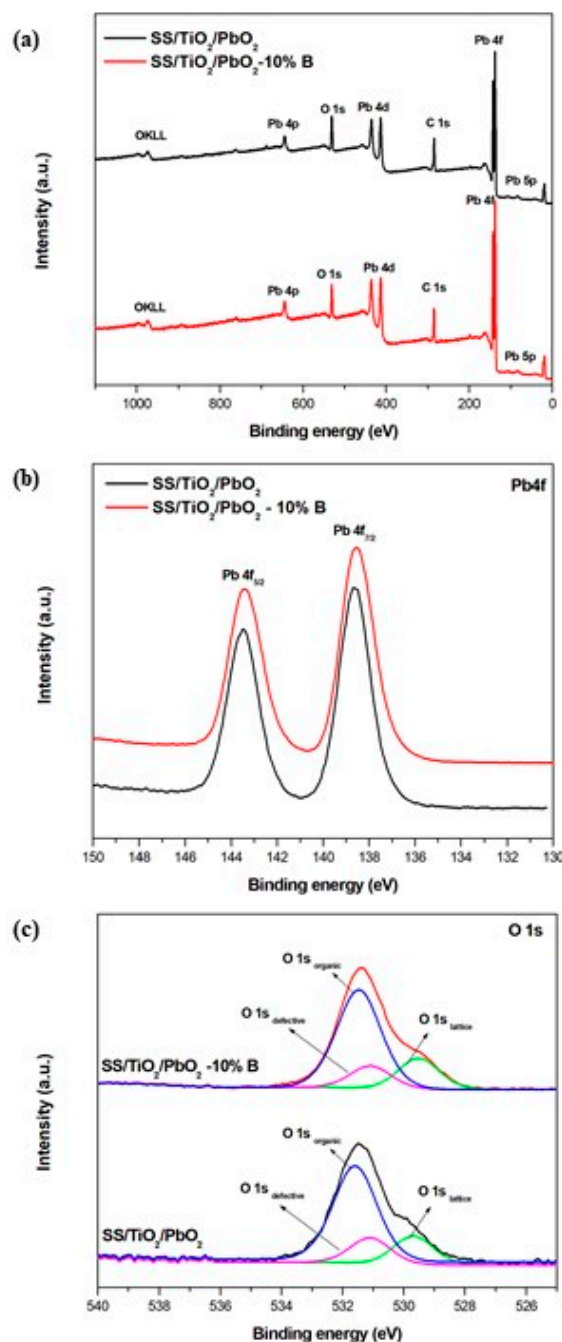


Figure 6. XPS spectrum of SS/TiO₂/PbO₂ and SS/TiO₂/PbO₂-10%B electrodes: (a) Wide scan spectrum, (b) O 1s Core-level spectrum, and (c) Pb 4f core-level spectrum.

Table 1. XPS data of different chemical states of O and Pb elements on the surface of SS/TiO₂/PbO₂ and SS/TiO₂/PbO₂-10%B electrodes.

Electrode	Binding Energy (eV)		O1s Organic (Atom%)	O1s Lattice (Atom%)	O1s Defective (Atom%)	O1s Lattice/O1s Defective (Atom%)	Pb4f _{7/2} /O1s Defective (Atom%)
	O1s Lattice	Pb4f _{7/2}					
SS/TiO ₂ /PbO ₂	529.69	138.87	16.07	4.44	4.06	1.09	3.70
SS/TiO ₂ /PbO ₂ -10%B	529.52	138.71	17.37	4.98	3.63	1.37	4.32

It can be seen from Figure 6b that the XPS spectrum of the Pb 4f core-level peak is formed by two contributions: the Pb 4f_{5/2} and the Pb 4f_{7/2} located, respectively, at 143.48 eV and 138.87 eV with a spin-orbit coupling of 4.9 eV. The Pb 4f_{7/2} can be attributed

to Pb^{2+} present in the lead oxide phase (Pb_3O_4) [47]. The XPS spectrum of O1s (Figure 5c) is deconvoluted into three peaks relative to the three chemical states of oxygen in the coating. The main peak, centered at an energy of 531.59 eV, corresponds to organic oxygen ($O1s_{organic}$), the second peak centered at an energy of 531.10 eV corresponds to defective O/-OH oxygen ($O1s_{defective}$), and the third peak at 529.52 eV is relative to the lattice oxygen ($O1s_{lattice}$) [14,15]. The $O1s_{lattice}$ could be assigned to strong oxygen binding (Pb-O bond) derived from the PbO_2 active layer [28,48,49]. The high binding energy of the organic oxygen is attributed to the adsorbed hydroxyl oxygen. The high content of $O1s_{organic}$ improves the catalytic performance of the electrode by providing more adsorbed reactive oxygen species (ROS), which in turn facilitates the degradation efficiency of the pollutant [50,51]. The percentage of $O1s_{organic}$ for the SS/ TiO_2 / PbO_2 -10%B anode (17.37%) is higher than that for the SS/ TiO_2 / PbO_2 anode (16.07%), indicating therefore that the doped PbO_2 coating has a higher electrocatalytic activity toward the degradation of the organic pollutant than the un-doped coating.

Table 1 shows the atomic percentage of different chemical elements present on the surface before and after doping. The obtained results reveal, on the one hand, a slight shift in the binding energies of the $O1s_{lattice}$ and $Pb\ 4f_{7/2}$ peaks toward low energies. On the other hand, we notice after doping the layers of 10% B an increase in the atomic percentage of the $O1s_{lattice}$ and a decrease in the atomic percentage of the $O1s_{defective}$. We also observe a decrease in the ratio between the atomic percentage of $O1s_{lattice}/O1s_{defective}$ and $Pb\ 4f_{7/2}/O1s_{defective}$. This means that defective (lacunar) oxide structures have been transformed into lattice oxide by the incorporation of boron into the defective structure of PbO_2 . Therefore, the changes at the $O1s_{lattice}$ peak are associated to the presence of boron dopant in lead dioxide lattice, which proves that boron atoms have been introduced into the active layer. Concerning the $Pb\ 4f_{7/2}$ core-level peak, the changes are attributed to the sensitivity of the lead atom to the chemical environment after the insertion of the dopant.

3.2. EIS Measurements and Fitting

EIS measurements were performed to further investigate the effect of the TiO_2 inter-layer and B dopant on the electrochemical properties of PbO_2 anodes. The EIS parameters listed in Table 2 were obtained from the collected experimental data fitted with the equivalent circuit (Figure 7) where R_s corresponds to the solution resistance, and ($R_{coating}, Q_{coating}$) and (R_{ct}, Q_{dl}) characterize, respectively, the properties of the coating and the charge transfer process at the interface electrode/electrolyte. The Warburg impedance (W) is assigned to the diffusion of charged species [12].

Table 2. EIS parameters obtained from fitting the electrical equivalent circuit on the experimental data of SS/ PbO_2 , SS/ TiO_2 / PbO_2 and SS/ TiO_2 / PbO_2 -10%B anodes.

	SS/ PbO_2	SS/ TiO_2 / PbO_2	SS/ TiO_2 / PbO_2 -10%B
R_s ($\Omega\ cm^2$)	480.6	64.71	104.5
$Q_{coating}$ ($S\ s^n\ cm^{-2}$)	5.80×10^{-6}	4.59×10^{-6}	22.8×10^{-6}
n	1	0.59	0.68
$R_{coating}$ ($\Omega\ cm^2$)	68.48	659	435.9
Q_{dl} ($S\ s^n\ cm^{-2}$)	16.8×10^{-6}	86.6×10^{-6}	74.3×10^{-6}
n	0.86	0.62	0.65
R_{ct} ($\Omega\ cm^2$)	3.18×10^6	3.76×10^4	5.64×10^4
W	4.01×10^{-6}	1.02×10^4	-

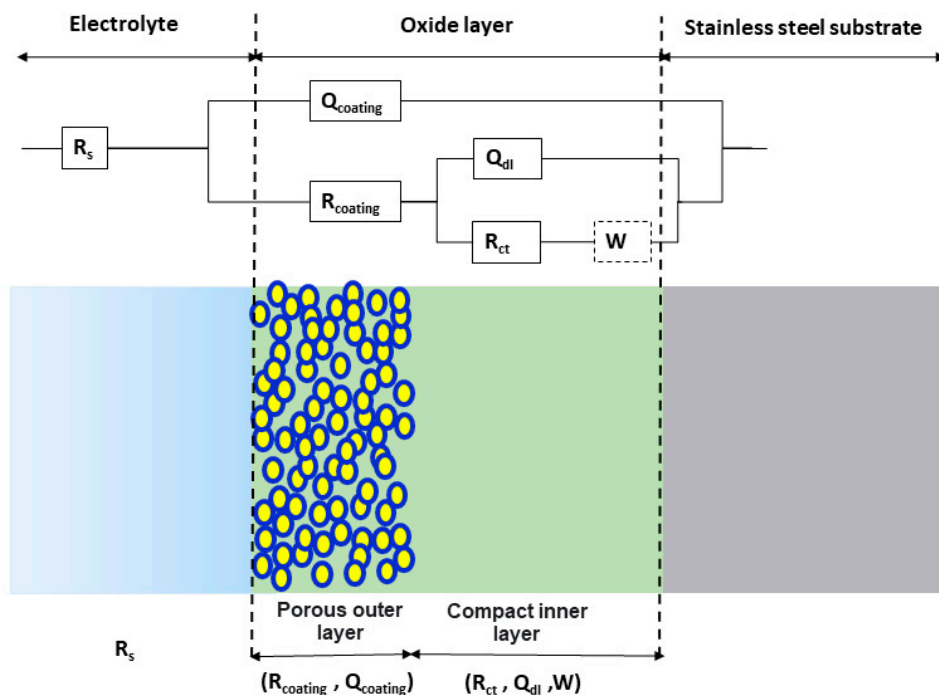


Figure 7. Schematic representation of equivalent circuit components used for modeling EIS data.

It can be seen from the Nyquist plots displayed in Figure 8 that SS/PbO₂ (Figure 8a) and SS/TiO₂/PbO₂-10%B (Figure 8c) electrodes present straight lines while SS/TiO₂/PbO₂ impedance spectra (Figure 8b) present a straight line with the appearance of a semi-circular shape at a high-frequency range attributed to the fast charge transfer at the anode interface [52]. The EIS responses shown in Table 2 indicate a significant difference in R_{ct} and R_{coating} values. The R_{ct} of SS/TiO₂/PbO₂ ($3.76 \times 10^4 \Omega \text{ cm}^2$) and SS/TiO₂/PbO₂-10%B ($5.64 \times 10^4 \Omega \text{ cm}^2$) anodes are smaller than the R_{ct} of SS/PbO₂ ($3.18 \times 10^6 \Omega \text{ cm}^2$) anode, and this is mainly explained by the compact structure and the small size of the crystalline particles of the B-doped PbO₂ coating demonstrated earlier with the SEM micrographs as well as by the improvement of the electronic conductivity with the B doping [46,53,54]. Therefore, we can say that the reduced charge transfer resistance induced by the introduction of an intermediate layer and by the B doping allows a faster electrochemical reaction rate [27] and could contribute to a lower power waste and a better current efficiency during the anodic oxidation process [15].

Concerning the R_{coating}, the resistance increased from 68.48 to 435.9 $\Omega \text{ cm}^2$ with, respectively, SS/PbO₂ and SS/TiO₂/PbO₂-10%B anodes. This result implies that the modified lead dioxide coating exhibits a better adhesion to the SS substrate by minimizing the transfer charge through the defects of coating. The intermediate layer contributed to strengthening the bonding between the electrode active layer and the substrate, which is reflected in the obtained values of coating resistance [55]. This high coating resistance leads to a lower punctual dissolution of the active layer and thus a longer lifetime of the developed anode [28].

3.3. Electrochemical Oxidation Performance of Electrodes

3.3.1. AMP Removal

In order to evaluate the electrocatalytic oxidation performance of the prepared anodes, HPLC analysis was carried out to identify AMP concentration during the electrochemical treatment, and COD removal rates were calculated at the end of the treatment since the COD is an indicator of the mineralization rate of organic matter including the initial polluting molecule as well as the by-products generated during the treatment.

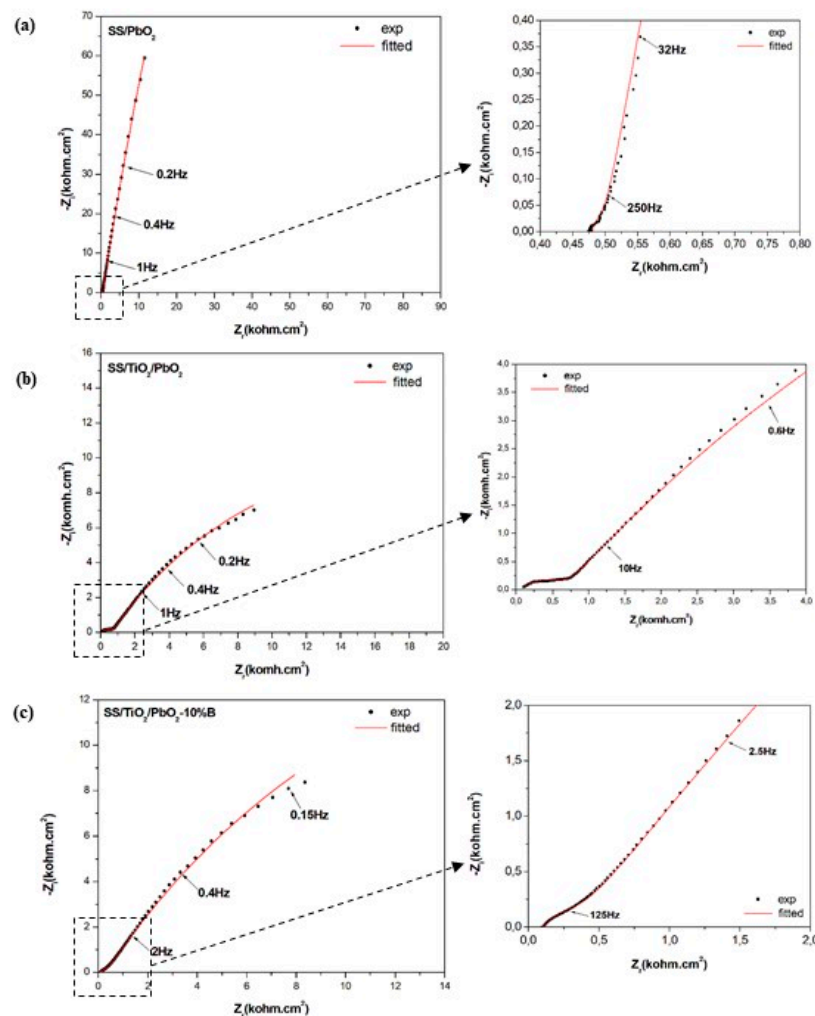
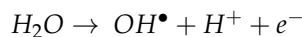


Figure 8. Nyquist impedance plots of (a) SS/PbO₂, (b) SS/TiO₂/PbO₂ and (c) SS/TiO₂/PbO₂-10%B anodes in 0.1 M Na₂SO₄ solution.

As shown in Figure 9, the AMP concentration decreased gradually as the electrochemical oxidation reaction proceeded, suggesting that SS/PbO₂, SS/TiO₂/PbO₂ and SS/TiO₂/PbO₂-10%B anodes exhibit efficient anode materials for the electrochemical degradation of AMP. Although the SS/PbO₂ anode showed the fastest degradation kinetics, it can be clearly seen that this anode had the lowest COD removal rate (30.77%) after 5 h of electrolysis compared to SS/TiO₂/PbO₂ and SS/TiO₂/PbO₂-10%B anodes which reached, respectively, 61.54% and 69.23%. Therefore, we can conclude that the addition of a TiO₂ intermediate layer and B doping of the PbO₂ active layer resulted in a better degradation of total organic compounds including ampicillin and the by-products that could be generated during the electrochemical treatment.

Since the electrochemical degradation process efficiency is mainly ascribed to the OH^\bullet radicals produced on the anode surface, the enhanced mineralization rate of the organic matter obtained with SS/TiO₂/PbO₂ and SS/TiO₂/PbO₂-10%B anodes could be explained by their strong hydroxyl radical generation ability [30,41]. This high hydroxyl radicals rate is attributed to the new physico-chemical properties of the electrode after the introduction of TiO₂ oxide film and the B doping of the outer layer. The small charge transfer resistance obtained with the modified PbO₂ anodes, demonstrated by impedance spectroscopy measurements, increased the conductivity of the coating and accelerated the charge transfer, which in turn promoted the water oxidation and the resultant OH^\bullet radicals generation [51]. The highest COD removal rate at the end of the electrolysis is reached by the B-doped PbO₂ electrode, and this is ascribed to the morphological difference at the electrode active

layer [30,52]. The compact structure of the SS/TiO₂/PbO₂-10%B anode (Figure 3c) formed by PbO₂ small particles provides a large active surface and therefore more active sites to generate more OH• radicals [24]. In addition to the crystal structure modification, B doping increases the conductivity by inducing sp² carbon impurities which influence the mineralization performance of the anode and enhance the electrogeneration of hydroxyl radicals OH• formed from water discharge on its surface [36,53].



The Fenton method is among the various advanced oxidation processes used to eliminate ampicillin where the antibiotic is completely eliminated within 2 min [56]. However, comparing to anodic oxidation, the pH solution is a parameter that affects Fenton reaction and may lead to ineffective Fenton oxidation in addition to the problem of iron sludge pollution treatment [57]. Concerning the anodic oxidation method, several anode materials were used for ampicillin degradation such as Ru-Ir-TiO₂ [58], Ti/TiO₂/PbO₂ [27] or boron-doped diamond [59] anodes where the pharmaceutical pollutant was totally eliminated after a short time of electrolysis. Despite the superior performance of these electrodes, they remain relatively expensive compared to the more affordable cost of the stainless steel substrate used in this study.

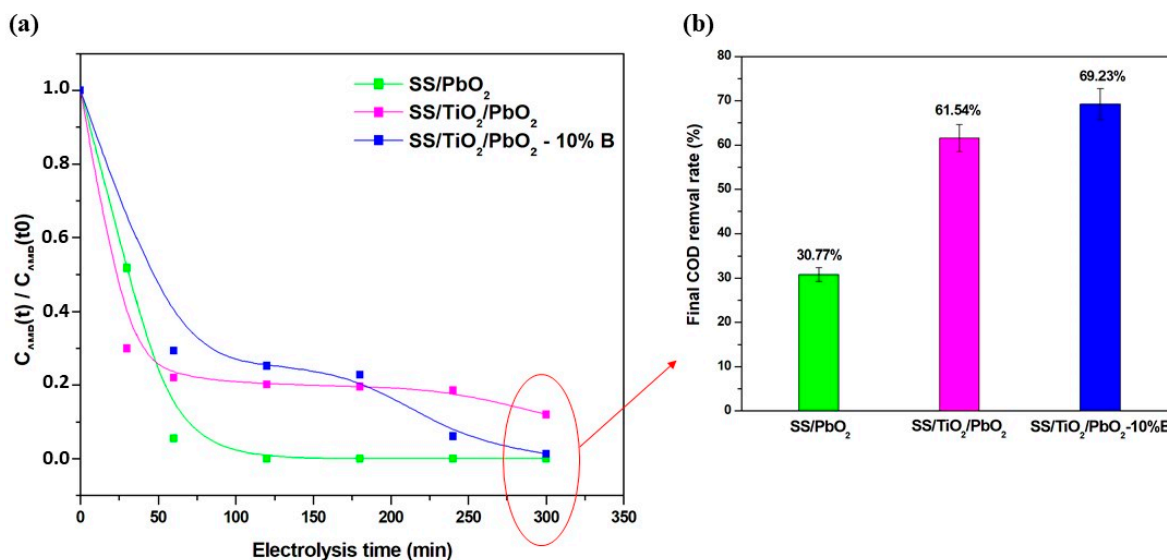


Figure 9. Evolution of ampicillin concentration during the electrochemical oxidation (a) and COD removal rate at the end of the treatment with the different PbO₂ anodes (b). Experimental conditions: C_{AMP} = 105 mg L⁻¹, j = 50 mA cm⁻², [Na₂SO₄] = 0.1 M.

3.3.2. Average Current Efficiency and Energy Evaluation

An evaluation of the efficiency of the treatment method in terms of average efficiency of the applied current (ACE) and consumed energy (EC) was also carried out in order to estimate the energy cost of the proposed optimized treatment.

The evolution trend of COD removal rate with the different anodes at the end of electrolysis is similar to that of the average current efficiency. As expected, the ACE values of SS/TiO₂/PbO₂ and SS/TiO₂/PbO₂-10%B were 53.60% and 60.30%, respectively, which were higher than those of the traditional SS/PbO₂ anode. These results are explained by the difference in the reactivity of the hydroxyl radicals electrogenerated on the anodes surfaces, which is influenced by the anode material [60].

The evolution of EC presented in Figure 10 shows that the consumed electric energy was about two times lower in the presence of the TiO₂ interlayer and B dopant. The EC values decreased from 0.125 to 0.056 kWh (g COD)⁻¹ with, respectively, SS/PbO₂ and SS/TiO₂/PbO₂-10%B electrodes. This decrease is due essentially to the high COD

removal rate achieved with SS/TiO₂/PbO₂-10%B during the last hour of treatment, since the higher the anode material electrocatalytic activity, the faster the electron transfer rate, and consequently, a large number of hydroxyl radicals can be generated. This leads to the lower energy consumption and lower energy cost of the electrochemical treatment process which represents, thus, a great advantage from an economic perspective [61,62].

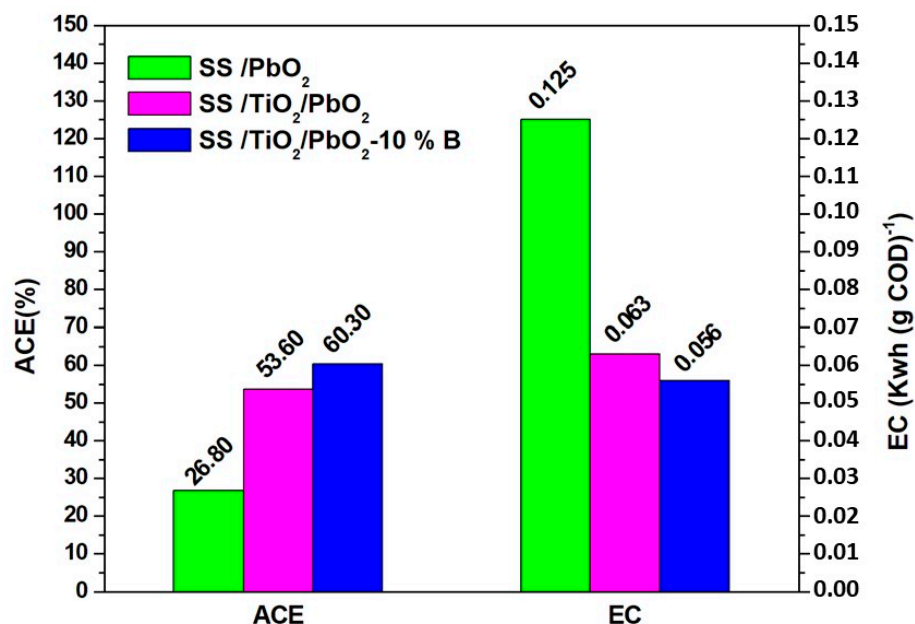


Figure 10. Evaluation of the average current efficiency (ACE) and the energy consumed (EC) at the end of the AMP electrolysis using SS/PbO₂, SS/TiO₂/PbO₂ and B-doped SS/TiO₂/PbO₂ anodes.

4. Conclusions

In this paper, a B-doped SS/TiO₂/PbO₂ anode was prepared on a stainless steel substrate by the sol-gel spin-coating method in order to study the electrochemical activity of the electrode toward the electrochemical degradation of a pharmaceutical pollutant.

Based on the morphological and structural characterization, we can say that the introduction of the TiO₂ inner layer and B doping of the PbO₂ outer layer provided a higher specific surface area which led to larger electrochemical active sites and promoted, consequently, the anodic oxidation reaction. In electrochemical measurements, the SS/TiO₂/PbO₂-10%B anode exhibited a smaller charge transfer resistance compared to the traditional SS/PbO₂ anode leading, therefore, to a higher hydroxyl radical generation capacity and a better electrochemical oxidation performance. The electrocatalytic degradation of AMP in aqueous solutions using modified PbO₂ anodes was investigated. The SS/TiO₂/PbO₂-10%B electrode had the highest oxidation ability with a widely higher COD removal efficiency (69.23%) than the SS/PbO₂ electrode (30.77%). Thus, the introduction of the TiO₂ intermediate layer and boron doping of the active layer represent two attractive methods to enhance the electrocatalytic activity and minimize the energy consumption of the PbO₂-based anode during the electrochemical treatment, making the SS/TiO₂/PbO₂-10%B electrode a promising anode for real applications in wastewater organic pollutants removal.

Author Contributions: Y.B.O.: conceptualization, methodology, investigation, writing—original draft. S.H.-G.: XPS measurement and analysis. D.B.: supervision, writing—review and editing. H.A.: supervision, writing—review and editing. All authors have read and agreed to the published version of the manuscript.

Funding: This research received no external funding.

Data Availability Statement: Not applicable.

Acknowledgments: This research was supported by Campus France (project PHC Utique 19G1202/41785XE) and the Tunisian Ministry of Higher Education and Scientific Research as part of a Tunisian national project. This paper is supported by the PRIMA programme under grant agreement No1923, project InTheMED. The PRIMA programme is supported by the European Union.



Conflicts of Interest: The authors declare no conflict of interest.

References

1. Majumder, A.; Gupta, B.; Gupta, A.K. Pharmaceutically Active Compounds in Aqueous Environment: A Status, Toxicity and Insights of Remediation. *Environ. Res.* **2019**, *176*, 108542. [[CrossRef](#)] [[PubMed](#)]
2. Olvera-Vargas, H.; Gore-Datar, N.; Garcia-Rodriguez, O.; Mutnuri, S.; Lefebvre, O. Electro-Fenton Treatment of Real Pharmaceutical Wastewater Paired with a BDD Anode: Reaction Mechanisms and Respective Contribution of Homogeneous and Heterogeneous [Rad]OH. *Chem. Eng. J.* **2021**, *404*, 126524. [[CrossRef](#)]
3. Moreira, F.C.; Boaventura, R.A.R.; Brillas, E.; Vilar, V.J.P. Electrochemical Advanced Oxidation Processes: A Review on Their Application to Synthetic and Real Wastewaters. *Appl. Catal. B Environ.* **2017**, *202*, 217–261. [[CrossRef](#)]
4. Titchou, F.E.; Zazou, H.; Afanga, H.; Gaayda, J.E.; Ait Akbour, R.; Nidheesh, P.V.; Hamdani, M. An Overview on the Elimination of Organic Contaminants from Aqueous Systems Using Electrochemical Advanced Oxidation Processes. *J. Water Process Eng.* **2021**, *41*, 102040. [[CrossRef](#)]
5. Garcia-Segura, S.; Keller, J.; Brillas, E.; Radjenovic, J. Removal of Organic Contaminants from Secondary Effluent by Anodic Oxidation with a Boron-Doped Diamond Anode as Tertiary Treatment. *J. Hazard. Mater.* **2015**, *283*, 551–557. [[CrossRef](#)]
6. Ben Osman, Y.; Le Meins, J.-M.; Bousselmi, L.; Akrou, H.; Berling, D. Effect of Electrode Shape and Deposition Technique on Electrochemical Treatment of Ampicillin in Water. *Environ. Technol. Innov.* **2021**, *23*, 101709. [[CrossRef](#)]
7. Sopaj, F.; Rodrigo, M.A.; Oturan, N.; Podvorica, F.I.; Pinson, J.; Oturan, M.A. Influence of the Anode Materials on the Electrochemical Oxidation Efficiency. Application to Oxidative Degradation of the Pharmaceutical Amoxicillin. *Chem. Eng. J.* **2015**, *262*, 286–294. [[CrossRef](#)]
8. Jiang, Y.; Zhao, H.; Liang, J.; Yue, L.; Li, T.; Luo, Y.; Liu, Q.; Lu, S.; Asiri, A.M.; Gong, Z.; et al. Anodic Oxidation for the Degradation of Organic Pollutants: Anode Materials, Operating Conditions and Mechanisms. A Mini Review. *Electrochem. Commun.* **2021**, *123*, 106912. [[CrossRef](#)]
9. Qiao, J.; Xiong, Y. Electrochemical Oxidation Technology: A Review of Its Application in High-Efficiency Treatment of Wastewater Containing Persistent Organic Pollutants. *J. Water Process Eng.* **2021**, *44*, 102308. [[CrossRef](#)]
10. Nurhayati, E. A Brief Review on Electro-Generated Hydroxyl Radical for Organic Wastewater Mineralization. *J. Sains Teknol. Lingkungan.* **2012**, *4*, 24–31. [[CrossRef](#)]
11. Kapalka, A.; Baltruschat, H.; Comninellis, C. Electrochemical Oxidation of Organic Compounds Induced by Electro-Generated Free Hydroxyl Radicals on BDD Electrodes. In *Synthetic Diamond Films: Preparation, Electrochemistry, Characterization, and Applications*; John Wiley & Sons, Inc.: Hoboken, NJ, USA, 2011; pp. 237–260. [[CrossRef](#)]
12. Elaissaoui, I.; Akrou, H.; Bousselmi, L. Interface Behavior of PbO₂ on Pure Lead and Stainless Steel as Anode for Dye Degradation. *Desalin. Water Treat.* **2016**, *57*, 16161–16176. [[CrossRef](#)]
13. Zhou, Q.; Zhou, X.; Zheng, R.; Liu, Z.; Wang, J. Application of Lead Oxide Electrodes in Wastewater Treatment: A Review. *Sci. Total Environ.* **2022**, *806*, 150088. [[CrossRef](#)]
14. Fu, X.; Han, Y.; Xu, H.; Su, Z.; Liu, L. Electrochemical Study of a Novel High-Efficiency PbO₂ Anode Based on a Cerium-Graphene Oxide Co-Doping Strategy: Electrodeposition Mechanism, Parameter Optimization, and Degradation Pathways. *J. Hazard. Mater.* **2022**, *422*, 126890. [[CrossRef](#)]
15. Yu, N.; Wei, J.; Gu, Z.; Sun, H.; Guo, Y.; Zong, J.; Li, X.; Ni, P.; Han, E. Electrocatalysis Degradation of Coal Tar Wastewater Using a Novel Hydrophobic Benzalacetone Modified Lead Dioxide Electrode. *Chemosphere* **2022**, *289*, 133014. [[CrossRef](#)]
16. Li, J.; Li, M.; Li, D.; Wen, Q.; Chen, Z. Electrochemical Pretreatment of Coal Gasification Wastewater with Bi-Doped PbO₂ Electrode: Preparation of Anode, Efficiency and Mechanism. *Chemosphere* **2020**, *248*, 126021. [[CrossRef](#)] [[PubMed](#)]
17. Feng, J.; Lan, H.; Tao, Q.; Chen, W.; Dai, Q. Electrochemical Oxidation of a Typical PPCP Wastewater with a Novel High-Efficiency PbO₂ Anode Based on NCNSs and Ce Co-Modification: Parameter Optimization and Degradation Mechanism. *J. Electroanal. Chem.* **2022**, *916*, 116305. [[CrossRef](#)]
18. Zhou, M.; Dai, Q.; Lei, L.; Ma, C.; Wang, D. Long Life Modified Lead Dioxide Anode for Organic Wastewater Treatment: Electrochemical Characteristics and Degradation Mechanism. *Environ. Sci. Technol.* **2005**, *39*, 363–370. [[CrossRef](#)]
19. Zhou, Y.; Li, Z.; Hao, C.; Zhang, Y.; Chai, S.; Han, G.; Xu, H.; Lu, J.; Dang, Y.; Sun, X.; et al. Electrocatalysis Enhancement of α , β -PbO₂ Nanocrystals Induced via Rare Earth Er(III) Doping Strategy: Principle, Degradation Application and Electrocatalytic Mechanism. *Electrochim. Acta* **2020**, *333*, 135535. [[CrossRef](#)]
20. Fazlinezhad, S.; Jafarzadeh, K.; Shooshtari Gugtaped, H.; Mirali, S.M. Characterization and Electrochemical Properties of Stable Ni²⁺ and F- Co-Doped PbO₂ Coating on Titanium Substrate. *J. Electroanal. Chem.* **2022**, *909*, 116145. [[CrossRef](#)]

21. Zhao, G.; Zhang, Y.; Lei, Y.; Baoying, L.V.; Gao, J.; Zhang, Y.; Li, D. Fabrication and Electrochemical Treatment Application of a Novel Lead Dioxide Anode with Superhydrophobic Surfaces, High Oxygen Evolution Potential, and Oxidation Capability. *Environ. Sci. Technol.* **2010**, *44*, 1754–1759. [[CrossRef](#)] [[PubMed](#)]
22. Elaissaoui, I.; Akrouit, H.; Grassini, S.; Fulginiti, D.; Bousselmi, L. Role of SiOx Interlayer in the Electrochemical Degradation of Amaranth Dye Using SS/PbO₂ Anodes. *Mater. Des.* **2016**, *110*, 633–643. [[CrossRef](#)]
23. Duan, X.; Li, J.; Liu, W.; Chang, L.; Yang, C. Fabrication and Characterization of a Novel PbO₂ Electrode with a CNT Interlayer. *RSC Adv.* **2016**, *6*, 28927–28936. [[CrossRef](#)]
24. Lin, H.; Niu, J.; Ding, S.; Zhang, L. Electrochemical Degradation of Perfluorooctanoic Acid (PFOA) by Ti/SnO₂-Sb, Ti/SnO₂-Sb/PbO₂ and Ti/SnO₂-Sb/MnO₂ Anodes. *Water Res.* **2012**, *46*, 2281–2289. [[CrossRef](#)]
25. Xing, X.; Ni, J.; Zhu, X.; Jiang, Y.; Xia, J. Maximization of Current Efficiency for Organic Pollutants Oxidation at BDD, Ti/SnO₂-Sb/PbO₂, and Ti/SnO₂-Sb Anodes. *Chemosphere* **2018**, *205*, 361–368. [[CrossRef](#)]
26. Tang, C.B.; Lu, Y.X.; Wang, F.; Niu, H.; Yu, L.H.; Xue, J.Q. Influence of a MnO₂-WC Interlayer on the Stability and Electrocatalytic Activity of Titanium-Based PbO₂ Anodes. *Electrochim. Acta* **2020**, *331*, 135381. [[CrossRef](#)]
27. Boukhchina, S.; Akrouit, H.; Berling, D.; Bousselmi, L. Highly Efficient Modified Lead Oxide Electrode Using a Spin Coating/Electrodeposition Mode on Titanium for Electrochemical Treatment of Pharmaceutical Pollutant. *Chemosphere* **2019**, *221*, 356–365. [[CrossRef](#)]
28. Yu, L.; Xue, J.; Zhang, L.; Tang, C.; Guo, Y. Fabrication of a Stable Ti/Pb-TiOxNWs/PbO₂ Anode and Its Application in Benzoquinone Degradation. *Electrochim. Acta* **2021**, *368*, 137532. [[CrossRef](#)]
29. Zhu, Y.; Jin, K.; Li, H.; Qian, H.; Wang, H.; Zhao, L. A Novel Anode with Anticorrosive Coating for Efficient Degradation of Toluene. *Chem. Eng. J.* **2018**, *334*, 206–215. [[CrossRef](#)]
30. Xia, Y.; Bian, X.; Xia, Y.; Zhou, W.; Wang, L.; Fan, S.; Xiong, P.; Zhan, T.; Dai, Q.; Chen, J. Effect of Indium Doping on the PbO₂ Electrode for the Enhanced Electrochemical Oxidation of Aspirin: An Electrode Comparative Study. *Sep. Purif. Technol.* **2020**, *237*, 116321. [[CrossRef](#)]
31. Dai, Q.; Zhou, J.; Weng, M.; Luo, X.; Feng, D.; Chen, J. Electrochemical Oxidation Metronidazole with Co Modified PbO₂ Electrode: Degradation and Mechanism. *Sep. Purif. Technol.* **2016**, *166*, 109–116. [[CrossRef](#)]
32. Bian, X.; Xia, Y.; Zhan, T.; Wang, L.; Zhou, W.; Dai, Q.; Chen, J. Electrochemical Removal of Amoxicillin Using a Cu Doped PbO₂ Electrode: Electrode Characterization, Operational Parameters Optimization and Degradation Mechanism. *Chemosphere* **2019**, *233*, 762–770. [[CrossRef](#)] [[PubMed](#)]
33. Chen, J.; Xia, Y.; Dai, Q. Electrochemical Degradation of Chloramphenicol with a Novel Al Doped PbO₂ Electrode: Performance, Kinetics and Degradation Mechanism. *Electrochim. Acta* **2015**, *165*, 277–287. [[CrossRef](#)]
34. He, Y.; Lin, H.; Guo, Z.; Zhang, W.; Li, H.; Huang, W. Recent Developments and Advances in Boron-Doped Diamond Electrodes for Electrochemical Oxidation of Organic Pollutants. *Sep. Purif. Technol.* **2019**, *212*, 802–821. [[CrossRef](#)]
35. Carolina Espinoza, L.; Candia-Onfray, C.; Vidal, J.; Salazar, R. Influence of the Chemical Nature of Boron-Doped Diamond Anodes on Wastewater Treatments. *Curr. Opin. Solid State Mater. Sci.* **2021**, *25*, 100963. [[CrossRef](#)]
36. Garcia-segura, S.; Vieira, E.; Martínez-huitle, C.A. Role of Sp³/Sp² Ratio on the Electrocatalytic Properties of Boron-Doped Diamond Electrodes: A Mini Review. *Electrochem. Commun.* **2015**, *59*, 52–55. [[CrossRef](#)]
37. Rodriguez-Mozaz, S.; Vaz-Moreira, I.; Varela Della Giustina, S.; Llorca, M.; Barceló, D.; Schubert, S.; Berendonk, T.U.; Michael-Kordatou, I.; Fatta-Kassinos, D.; Martinez, J.L.; et al. Antibiotic Residues in Final Effluents of European Wastewater Treatment Plants and Their Impact on the Aquatic Environment. *Environ. Int.* **2020**, *140*, 105733. [[CrossRef](#)]
38. Boge, E.A.; Nyongesa, P.; Okoth, P.; Sifuna, A.W. Biofilms and Antimicrobial Susceptibility Profiles of Escherichia Coli Recovered from Wastewater Treatment Plants in Kakamega Municipality, Kenya. *Egypt. J. Microbiol.* **2021**, *56*, 25–34. [[CrossRef](#)]
39. Stachurová, T.; Píková, H.; Bartas, M.; Semerád, J.; Svobodová, K.; Malachová, K. Beta-Lactam Resistance Development during the Treatment Processes of Municipal Wastewater Treatment Plants. *Chemosphere* **2021**, *280*, 130749. [[CrossRef](#)]
40. Zafar, R.; Bashir, S.; Nabi, D.; Arshad, M. Occurrence and Quantification of Prevalent Antibiotics in Wastewater Samples from Rawalpindi and Islamabad, Pakistan. *Sci. Total Environ.* **2021**, *764*, 142596. [[CrossRef](#)]
41. Boukhchina, S. Elaboration Des Anodes Par Différentes Méthodes de Dépôt et Leur Application Dans La Dépollution Des Eaux Usées Par Voie Electrochimique. Ph.D. Thesis, Université de Carthage, Carthage, Tunisie, 2021.
42. Ben Osman, Y. Traitement Electrochimique Des Eaux Usées Chargées En Polluants Émergents Utilisant Des Anodes Innovantes à Coût Maîtrisé. Ph.D. Thesis, Université de Haute-Alsace, Mulhouse, France, 2022.
43. AFNOR Norme Française NF T 90-101 (Février 2001): Qualité de l'eau: Détermination de La Demande Chimique En Oxygène (DCO); AFNOR: Paris, France, 2001.
44. Elaissaoui, I.; Akrouit, H.; Bousselmi, L. Electrochemical Degradation of Dye on Lead Dioxide Electrodeposited on Stainless Steel: Effect of Cyclic Voltammetry Parameters. *Desalin. Water Treat.* **2016**, *57*, 22120–22132. [[CrossRef](#)]
45. Ghazouani, M.; Akrouit, H.; Bousselmi, L. Nitrate and Carbon Matter Removals from Real Effluents Using Si/BDD Electrode. *Environ. Sci. Pollut. Res.* **2017**, *24*, 9895–9906. [[CrossRef](#)] [[PubMed](#)]
46. Yang, C.; Shang, S.; Li, X. Fabrication of Sulfur-Doped TiO₂ Nanotube Array as a Conductive Interlayer of PbO₂ Anode for Efficient Electrochemical Oxidation of Organic Pollutants. *Sep. Purif. Technol.* **2021**, *258*, 118035. [[CrossRef](#)]
47. Kim, K.S.; O'Leary, T.J.; Winograd, N. X-Ray Photoelectron Spectra of Lead Oxides. *Anal. Chem.* **1973**, *45*, 2214–2218. [[CrossRef](#)]

48. Velichenko, A.B.; Amadelli, R.; Zucchini, G.L.; Girenko, D.V.; Danilov, F.I. Electrosynthesis and Physicochemical Properties of Fe-Doped Lead Dioxide Electrocatalysts. *Electrochim. Acta* **2000**, *45*, 4341–4350. [[CrossRef](#)]
49. Liu, Y.; Liu, H.; Ma, J.; Li, J. Investigation on Electrochemical Properties of Cerium Doped Lead Dioxide Anode and Application for Elimination of Nitrophenol. *Electrochim. Acta* **2011**, *56*, 1352–1360. [[CrossRef](#)]
50. Feng, J.; Tao, Q.; Lan, H.; Xia, Y.; Dai, Q. Electrochemical Oxidation of Sulfamethoxazole by Nitrogen-Doped Carbon Nanosheets Composite PbO₂ Electrode: Kinetics and Mechanism. *Chemosphere* **2022**, *286*, 131610. [[CrossRef](#)]
51. Yu, S.; Hao, C.; Li, Z.; Zhang, R.; Dang, Y.; Zhu, J.J. Promoting the Electrocatalytic Performance of PbO₂ Nanocrystals via Incorporation of Y₂O₃ Nanoparticles: Degradation Application and Electrocatalytic Mechanism. *Electrochim. Acta* **2021**, *369*, 137671. [[CrossRef](#)]
52. Wei, F.; Liao, D.; Lin, Y.; Hu, C.; Ju, J.; Chen, Y.; Feng, D. Electrochemical Degradation of Reverse Osmosis Concentrate (ROC) Using the Electrodeposited Ti/TiO₂-NTs/PbO₂ Electrode. *Sep. Purif. Technol.* **2021**, *258*, 118056. [[CrossRef](#)]
53. Bogdanowicz, R.; Fabiańska, A.; Golunski, L.; Sobaszek, M.; Gnyba, M.; Ryl, J.; Darowicki, K.; Ossowski, T.; Janssens, S.D.; Haenen, K.; et al. Influence of the Boron Doping Level on the Electrochemical Oxidation of the Azo Dyes at Si/BDD Thin Film Electrodes. *Diam. Relat. Mater.* **2013**, *39*, 82–88. [[CrossRef](#)]
54. dos Santos, A.J.; Fortunato, G.V.; Kronka, M.S.; Vernasqui, L.G.; Ferreira, N.G.; Lanza, M.R.V. Electrochemical Oxidation of Ciprofloxacin in Different Aqueous Matrices Using Synthesized Boron-Doped Micro and Nano-Diamond Anodes. *Environ. Res.* **2022**, *204*, 112027. [[CrossRef](#)]
55. Hu, Z.; Cai, J.; Song, G.; Tian, Y.; Zhou, M. Anodic Oxidation of Organic Pollutants: Anode Fabrication, Process Hybrid and Environmental Applications. *Curr. Opin. Electrochem.* **2021**, *26*, 100659. [[CrossRef](#)]
56. Elmolla, E.S.; Chaudhuri, M. Degradation of the Antibiotics Amoxicillin, Ampicillin and Cloxacillin in Aqueous Solution by the Photo-Fenton Process. *J. Hazard. Mater.* **2009**, *172*, 1476–1481. [[CrossRef](#)]
57. Jiang, Y.; Ran, J.; Mao, K.; Yang, X.; Zhong, L.; Yang, C.; Feng, X.; Zhang, H. Recent Progress in Fenton/Fenton-like Reactions for the Removal of Antibiotics in Aqueous Environments. *Ecotoxicol. Environ. Saf.* **2022**, *236*, 113464. [[CrossRef](#)]
58. Wirzal, M.D.H.; Yusoff, A.R.M.; Zima, J.; Barek, J. Degradation of Ampicillin and Penicillin G Using Anodic Oxidation. *Int. J. Electrochem. Sci.* **2013**, *8*, 8978–8988.
59. Frontistis, Z.; Mantzavinos, D.; Meriç, S. Degradation of Antibiotic Ampicillin on Boron-Doped Diamond Anode Using the Combined Electrochemical Oxidation—Sodium Persulfate Process. *J. Environ. Manag.* **2018**, *223*, 878–887. [[CrossRef](#)]
60. Panizza, M.; Cerisola, G. Influence of Anode Material on the Electrochemical Oxidation of 2-Naphthol: Part 2. Bulk Electrolysis Experiments. *Electrochim. Acta* **2004**, *49*, 3221–3226. [[CrossRef](#)]
61. Ghazouani, M.; Akrouf, H.; Jellali, S.; Bousselmi, L. Comparative Study of Electrochemical Hybrid Systems for the Treatment of Real Wastewaters from Agri-Food Activities. *Sci. Total Environ.* **2019**, *647*, 1651–1664. [[CrossRef](#)]
62. Guo, Z.; Zhang, Y.; Jia, H.; Guo, J.; Xia, M.; Wang, J. Electrochemical Methods for Landfill Leachate Treatment: A Review on Electrocoagulation and Electrooxidation. *Sci. Total Environ.* **2022**, *806*, 150529. [[CrossRef](#)]

Disclaimer/Publisher's Note: The statements, opinions and data contained in all publications are solely those of the individual author(s) and contributor(s) and not of MDPI and/or the editor(s). MDPI and/or the editor(s) disclaim responsibility for any injury to people or property resulting from any ideas, methods, instructions or products referred to in the content.